

Estimation of the Size of Earthquake Preparation Zones

By I. P. DOBROVOLSKY, S. I. ZUBKOV and V. I. MIACHKIN¹

Abstract – During the earthquake preparation a zone of cracked rocks is formed in the region of a future earthquake focal zone under the influence of tectonic stresses. In the study of the surrounding medium this region may be considered as a solid inclusion with altered moduli. The inclusion appearance causes a redistribution of the stresses accompanied by corresponding deformations. This paper deals with the study of deformations at the Earth's surface, resulting from the appearance of a soft inclusion.

The Appendix contains an approximate solution of the problem for a soft elastic inclusion in an elastic half-space. It is assumed that the moduli of the inclusion differ slightly from those of the surrounding medium (by no more than 30%). The solution permits us to calculate the deformations at the Earth's surface for the inclusion with an arbitrary heterogeneity and anisotropy. The problem is solved by the small perturbation method.

The calculation is made for a special case of a homogeneous isotropic inclusion where only the shear modulus decreases. The shear stresses act at infinity. The equations are deduced for the estimation of deformations and tilts at the Earth's surface as a function of the magnitude of the preparing earthquake and the distance from the epicentre. Comparison has shown a satisfactory agreement between the theoretical and field results. Let us assume that the zone of effective manifestation of the precursor deformations is a circle with the centre in the epicentre of the preparing earthquake. The radius of this circle called 'strain radius' may be calculated from the equation

$$\rho = 10^{0.43M} \text{ km,}$$

where M is the magnitude.

It was shown that the precursors of other physical nature fall into this circle.

Key words: Earthquake prediction; Earthquake precursory models; Strain accumulation.

1. Introduction

To ensure a proper organisation of the work on earthquake prediction it is extremely important to estimate the size and shape of the earthquake preparation zone. There is no doubt now that a network of stations is necessary for recording the precursor phenomena with a single computing centre for processing all the data. However, many controversial questions still remain concerning the density of the station network and the principles of processing the obtained information. It is

¹ Institute of Physics of the Earth, Academy of Science, Moscow, USSR.

obvious that the network density will depend upon the magnitude of the preparing earthquake which we intend to 'catch'. Just here the estimations of the preparation zone *size* will be useful. The estimates of the possible preparation zone *shape* may be used as a basis for the elaboration of an algorithm to process the obtained information. Another aspect of the problem is connected with the analysis of the precursors of the earthquake that had already happened. In this case the coincidence in time was usually first of all taken into account and almost no attention paid to the discussion of the correlation between the precursor intensity, its epicentral distance and the attending seismic conditions in the precursor region. Good estimates of the precursor zone size may give rise to useful doubts permitting us to establish whether the recorded distant and intensive precursors do belong to the particular investigated earthquake.

This paper deals with theoretical studies of the deformations at the Earth's surface arising during the earthquake preparation. Our considerations are based on certain concepts of the earthquake preparation process.

In [1] two most popular preparation models were investigated: the dilatancy-diffusion model (DD) which is widely quoted in the U.S.A., and the model developed in the Institute of Physics of the Earth (U.S.S.R.), hereafter called the IPE-model.

According to the DD-model a porous cracked saturated rock constitutes the initial medium. With the increase of the tectonic stresses the cracks extend as well and disengagement cracks appear near the pores, the favourably oriented cracks being opened. Water flows into the opened cracks drying the rock near each pore. This results in decrease of pore pressure in the total preparation zone and water diffusion into the zone from the surrounding medium. The return of pore pressure and crack increase bring about a main rupture at the end of the diffusion period.

According to the IPE-model the process is as follows. A cracked rock zone (i.e. a focal zone) is formed by the increasing tectonic stresses. The shape and volume of this focal zone change slowly with time. A complicated process of crack birth, growth, healing and redistribution proceeds within the zone. At a certain stage the focal zone volume, crack concentration and size reach such values that the whole 'construction' (focal zone) becomes unstable. The cracks quickly concentrate near the fault surface where the main rupture has passed.

Comparing both theories even on the basis of very brief descriptions we can reveal at least one common principle: at a certain preparation stage a region with many cracks is formed. In the study of the behaviour of the medium outside this cracked region, for instance at the Earth's surface, we can neglect the detailed structure of the focal region. The surrounding medium perceives the focal region as a *solid soft inclusion*.

The concept of the preparation region as a soft inclusion can be found in the works of BRADY [2, 3]. Such a model permitted him to explain qualitatively many phenomena, but he did not give estimates of the preparation zone size. The solution of the problem for the soft inclusion in the rock sample was obtained in [2] by finite element method.

It is obvious that before starting a detailed study of the problems connected with the soft inclusion we must be convinced that this concept does not contradict the field observations. Evidently, the most convincing confirmation is the phenomenon of the velocity change of the seismic waves passing through the preparation zone. This question was widely discussed in the literature but we shall mention only the early publications. Changes in the times of the longitudinal wave propagations were reported in 1950 by HAYAKAWA [4]. The work [5] shows the Poisson's ratio changes before and after the earthquake. Systematic investigations carried out by Soviet seismologists in Garm (Tajikistan) have definitely established the phenomenon of the changes in the seismic wave propagation times prior to earthquakes.

The problem of the soft inclusion was also considered in several other publications [8, 10]. ESHELBY [8] has studied an elastic isotropic homogeneous inclusion of ellipsoidal form.

The investigations of BERGER and BEAUMONT [9, 10] are similar to our work. These authors using the finite element method have solved the problem of an elastic isotropic homogeneous dilatant zone 20×40 km, with its third dimension extending along the 30° parallel of the northern latitude on a spherically symmetrical Earth model. They showed curves for the solid earth tide displacements, strains and tilts inside and outside the inclusion. It is shown that these data may be used for earthquake prediction. However in the previous studies [8, 10] no correlation between the preparing earthquake magnitude and the amplitude of the premonitory deformations was established.

The above-mentioned analysis permitted us to formulate the requirements for the solution of the soft inclusion problem. Firstly we must have an analytical solution since on its basis it is most convenient to develop the asymptotic formula for the simple estimates. Secondly, the possible anisotropy and heterogeneity of the inclusion (the anisotropy resulting from the crack orientation in the inclusion) are to be taken into account in the solution.

We have found an approximate solution of the problem of the soft inclusion in the half-space [11]. It meets the above-mentioned requirements, but is only suitable for small modulus differences (apparently no more than 30%). A more detailed solution description is given in the Appendix. It is to be noted that we pay much attention to the study of the deformation distribution. We think it is important for the following reasons.

(a) The deformations are the tensor components and the tilts are the vector components. Therefore these values may be connected with the direction towards the epicentre.

(b) The mechanical processes of earthquake preparation are always accompanied by deformations. The precursors of another physical nature often require for their manifestation a complex of specific natural conditions.

(c) Apparently the deformations are the primary phenomena. We think that in most cases the manifestation of the precursors of non-mechanical nature is caused

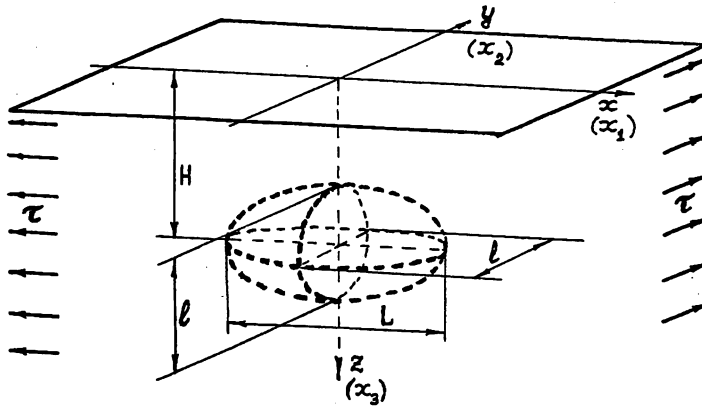


Figure 1
Inclusion in a half-space.

(under favourable conditions) just by the surrounding medium deformation. However, we realise that this concept is hypothetical.

2. Calculation of the surface deformations during the earthquake preparation

We shall use here the results of the solution for an elastic inclusion in the elastic half-space, as described in the Appendix.

Let the half-space $z \geq 0$ (Fig. 1) be at infinity under the action of homogeneous shear stresses. The surface $z = 0$ is stress-free. The appearance of the soft inclusion at the Earth's surface brings about deformations and tilts that can be calculated for a homogeneous isotropic inclusion according to equations (20)–(26). These formulae were derived proceeding from the assumption that the bulk modulus does not change while the shear modulus μ shows a relative decrease $\alpha = \Delta\mu/\mu$. Equations (20)–(26) involve the product αV where V is the inclusion volume. The estimation of these values as functions of the earthquake magnitude is the most important stage in the solution of our problem.

The value α can be estimated from the elastic wave velocity changes. We assume α to be independent of magnitude because the amount of the velocity changes observed seem to be constant (e.g., 6). Proceeding from the theoretical concepts of the earthquake preparation this can be qualitatively explained as follows. According to the DD-model the crack concentration and size are independent of the magnitude, i.e., the weakening of the inclusion material is the same for all earthquakes. In the IPE-model all earthquakes are prepared similarly, i.e., the crack size and concentration remain unchanged relative to the future focal zone, hence the effective inclusion moduli are similar.

SHEBALIN [12] has shown that the focal zone of the crustal earthquake with $M \geq 5$ can be considered as a rupture that has the shape of an ellipse with axes $L =$

$10^{(0.7M-2.8)}$ km and $l = 10^{(0.3M-0.8)}$ km, where M is the magnitude. At $M < 5$ $L = l = 10^{(0.5M-1.8)}$ km. Our main assumption is as follows. We assume the volume V corresponding to the maximum αV to be an ellipsoid formed by rotation of the rupture ellipse about the major axis L . Then

$$V = \frac{\pi}{6} L l^2 = \frac{\pi}{6} 10^{1.3M-4.4} \text{ km}^3 \quad \text{at } M \geq 5, \quad (\text{A})$$

$$V = \frac{\pi}{6} l^3 = \frac{\pi}{6} 10^{1.5M-5.4} \text{ km}^3 \quad \text{at } M < 5.$$

Now we can enter into details of the Earth's surface deformation. The deformations and tilts are calculated according to equation (20). They are symmetrical and anti-symmetrical relative to the coordinate axes. Hence, it is enough to study their behaviour in the first quadrant. The deformation fields have a complicated structure.

As an example let us consider the e_{xx} deformations, calculated according to the first part of equation (20) and represent the said deformations in a non-dimensional form.

Assuming

$$R = \frac{l}{2}, \quad \xi = \frac{x}{R}, \quad \eta = \frac{y}{R}, \quad h = \frac{H}{R}$$

and that the half-space is subjected to constant shear stress we obtain the deformation in a non-dimensional form

$$\omega_{xx} = \frac{2\pi\mu R^3}{\alpha V \tau} e_{xx}.$$

Figures 2, 3 and 4 show the isolines of ω_{xx} deformations for $h = 1, 3, 5$, respectively. The inclusion epicentre is to be found at the origin of the coordinates. From these figures it is evident that in the near zone the field changes appreciably with depth. At long distances the deformation behaviour is almost similar. On the coordinate axes and at the borderline between the positive and negative values the deformations approach zero. Therefore the strain gauge theoretically cannot detect the longitudinal deformation e_{xx} at any distance from the epicentre.

However, our object is to estimate the zone of the greatest deformation extension. The question to be answered is as follows: what is the greatest distance ρ_ε at which the deformation with a given value ε can be detected. In Figs. 2, 3 and 4 the arrow indicates the distance ρ_ε for $\omega_{xx} = 10^{-4}$. This distance is measured in a quite definite direction depending on the shear stress direction. If the stress direction is unknown we can with an equal probability detect the deformation ε at the distance ρ_ε in any arbitrary direction. Then the circle with a ρ_ε radius shall represent the zone where a deformation equal to or exceeding ε can appear. This is sought to be the manifestation zone of the premonitory deformations. We shall call the value ρ_ε the strain radius, the latter being the greatest distance from the epicentre where the deformation with a given

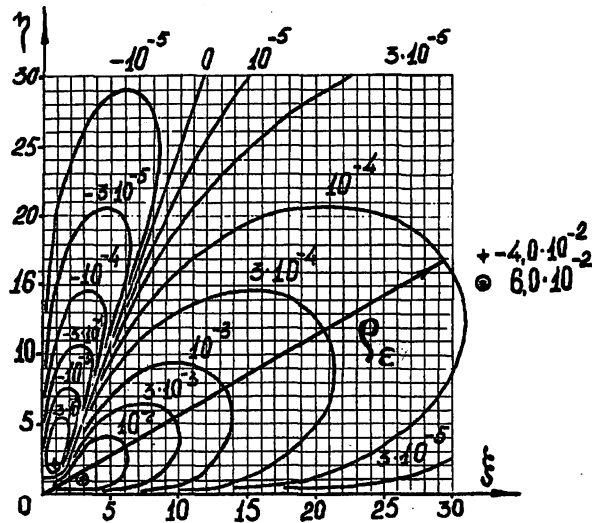


Figure 2
Conventional deformation ω_{xx} at $h = 1$.

value ε is detected. From Figs. 2, 3 and 4 it is evident that ρ_ε increases as the hypocentre depth decreases. Hence the upper estimate for ρ_ε can be obtained at $H \rightarrow 0$. This is shown in the Appendix. Equation (25) gives

$$\rho_\varepsilon = 0.85 \sqrt[3]{\frac{\alpha V \tau}{\mu \varepsilon}}, \tag{B}$$

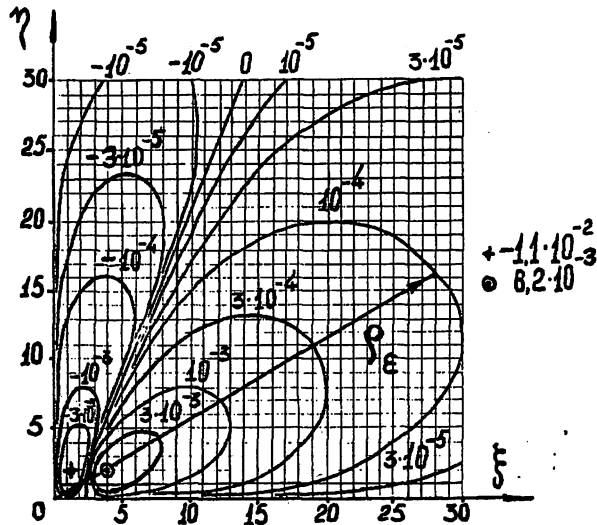


Figure 3
Conventional deformation ω_{xx} at $h = 3$.

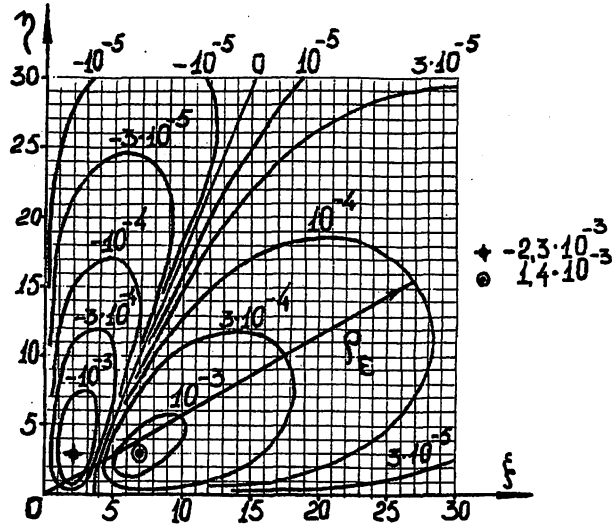


Figure 4
Conventional deformation ω_{xx} at $h = 5$.

where ε is the greatest principal deformation in the absolute value. It is interesting to note that the tilt radius (equation (26)) is smaller than the strain radius. The same result was obtained by others [9, 10]. The peculiarity of the equation (B) is that all values fall under the cube root. The change of a value by one order will bring about only a two-fold change in the ρ_ε distance. This means that the variation of the under-root expression even in large scale shall almost not change the ρ_ε value. Consequently the formula shall give either a result close to the true one or a wrong result hard to 'correct'.

To obtain concrete estimates let us assume V according to equation (A), $\tau = 10^9$ bar, $\mu = 2 \times 10^5$ bar, $\alpha = 0.1$ (this corresponds to the velocity change by no more than 5%). Then

$$\rho_\varepsilon = \frac{10^{0.433 M - 2.73}}{\sqrt[3]{\varepsilon}} \text{ km} \quad M \geq 5, \tag{C}$$

$$\rho_\varepsilon = \frac{10^{0.5 M - 3.06}}{\sqrt[3]{\varepsilon}} \text{ km} \quad M < 5.$$

The calculations show a small difference between the two equations (C), this difference making 34% for $M = 3$ and 15% for $M = 4$. For our estimates we can certainly neglect the said fact and use only the upper equation (C), from which we obtain for different deformation values

$$\begin{aligned} \rho_{-10} &= 10^{0.433 M + 0.60} \text{ km} \quad \text{at } \varepsilon = 10^{-10} \\ \rho_{-9} &= 10^{0.433 M + 0.27} \text{ km} \quad \text{at } \varepsilon = 10^{-9} \\ \rho_{-8} &= 10^{0.433 M - 0.06} \text{ km} \quad \text{at } \varepsilon = 10^{-8} \\ \rho_{-7} &= 10^{0.433 M - 0.40} \text{ km} \quad \text{at } \varepsilon = 10^{-7} \end{aligned}$$

Equation (C) is valid when ρ_ε is no less than three times the mean focal zone size.

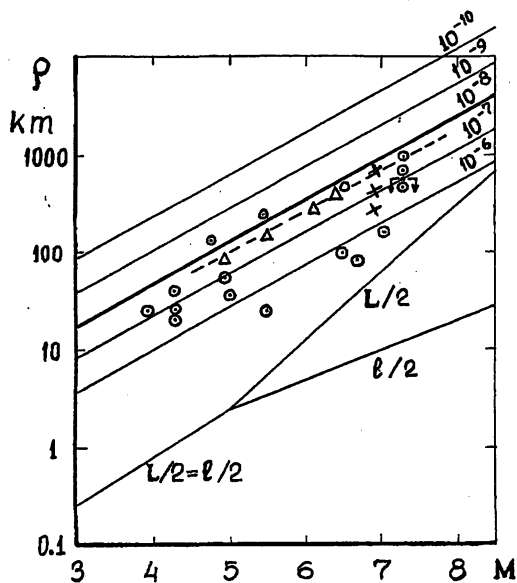


Figure 5

The precursor epicentral distance versus the magnitude of an earthquake. \odot , geochemical precursors [14–20]; ----, resistance [24]; \times , resistance [21]; Δ , telluric current [22, 23]; \square with arrows, radon [21]; \circ , light effects [13].

3. Comparison with the observed data and discussion of the results

Figure 5 shows the lines for the relationship between the strain radius and magnitude for the strains from 10^{-6} to 10^{-10} (five continuing parallel straight lines). The branched line characterises the earthquake focal zone sizes. The same figure also contains the points showing the various precursor anomalies. The results for the deformations and tilts are given in Table 1 and are not plotted in Fig. 5.

We suppose that the joint analysis of the precursors of different physical nature and of the obtained theoretical results permits us to make well-founded recommendations in respect to the precursor manifestation zone size in general.

The light phenomena [13] arose just before the earthquake and accompanied it. The plotted point shows the greatest extension of the phenomenon.

The most numerous are the data on the geochemical precursors [14–20]. They show the anomalies in radon, helium, carbon dioxide, hydrogen, fluorine and chlorine content some days before the earthquake. The changes were in the order of tens and hundreds of percents. Of greatest interest are the data described in reference [21] on the radon content change (the point with two arrows). This point corresponds to the maximum extension of this effect. The data obtained on the basis of the telluric current variations are taken from references [22, 23].

Of interest are the data on the variation of the resistance. Three points are adopted from reference [21]. They correspond to resistance variations by 10%, 4%, and 0%, i.e., the most distant point shows the distance limit of detectability. The dashed line taken

from the work [24] is drawn using the same principle. Its author has treated 21 observations of the resistance variations (12 values being obtained after and 9 values prior to the earthquake). The empirical straight line shows the effect extension border. It is to be noted that this straight line has the same slope as our straight lines.

Summarizing the discussion of Fig. 5 we can say that the manifestation zone of all mentioned precursors is limited by a straight line that coincides practically with the strain radius for a deformation of 10^{-8} .

In Table 1 the observed data are compared with the calculated values for the precursor tilts and strains. Almost all values are adopted from the work [25] and supplemented with the data presented in [26–31].

The theoretical epicentral distance indicated in Table 1 was computed using equation (C), i.e. as a greatest distance where the given strain (or tilt) value reveals itself. Hence we should note a satisfactory agreement between the theoretical and observed values when the theoretical value is more than or equal to that observed. Of the indicated data on 24 earthquakes 13.5 meet this requirement (earthquake No. 11 meeting this requirement only by half). It is interesting to note that of 14 earthquakes which happened in Japan a satisfactory agreement was found for 11.5 (82%). Most frequently the long distances are to be found in the works of the Soviet seismologists.

It is to be noted that certain data are doubtful. For instance, the author of the data on earthquakes 15, 16 and 17 [31] stated that of 127 earthquakes recorded in 1957–65 only the above-mentioned had marked precursor tilts. In earthquake 17 devices were installed on the fault. It is also very difficult to be sure of reliability of the precursors on the basis of the work [30]. This work involves a seismogram 5 hours 'long' prior to the earthquake. No analysis of background noise variations is presented in the work.

It should be added that for the majority of the above-mentioned earthquakes the depth of the hypocentre is unknown. Our estimates were obtained for shallow earthquakes but may be wrong for other conditions.

The analysis carried out for strains and tilts is quite incomplete. Detailed investigations in this direction present a separate problem.

In some cases the agreement between the theoretical estimates and the observations is satisfactory, in other cases it may be that unreliable observations could be identified as such if our theoretical model can be substantiated.

The estimates of the precursor region size are also presented in the works of RIKITAKE [32, 33]. Using DAMBARA's formula [34] Rikitake determined the radius of a premonitory deformation zone $r = 10^{0.51M - 2.27}$. In [35] it is shown that this formula describes the size of the zones of intensive deformation (about 10^{-5}). In the work [36] the estimate of the premonitory deformation region was obtained by extrapolation of the data reported in [7] to the region of large magnitudes. The analysis has revealed

Table 1

No.	Earthquake area (country)	Year	Magnitude	Tilt or deformation value	Time prior to the earthquake (twenty-four hours)	Epicentral distance		Source
						observed	theoret.	
1.	Japan	1923	7.9	1.5×10^{-5}	0.33	80	126	[25]
2.	Japan	1943	7.4	5×10^{-7}	0.25	60	237	[25]
3.	Japan	1944	8.0	2×10^{-7}	0.24	160	586	[25]
4.	Japan	1950	6.7	7.5×10^{-7}	0.29	80	103	[25]
				2×10^{-7}	0.28	120	160	
				1×10^{-7}	0.23	200	202	
5.	Japan	1952	6.8	3×10^{-4}	90	40	15	[25]
				1×10^{-4}	10	40	22	
6.	Japan	1952	7.0	3×10^{-6}	15	80	88	[25]
				1×10^{-6}	15	60	126	
				1×10^{-6}	15	80	126	
				2.5×10^{-6}	300	50	147	
				1.5×10^{-6}	120	72	174	
				3×10^{-6}	60	72	138	
				1×10^{-6}	11	72	199	
				3×10^{-6}	200	40	32	[25]
7.	Japan	1960	6.0	5×10^{-6}	100	40	27	
				3×10^{-6}	10	40	32	
				1.5×10^{-5}	120	90	19	
				2×10^{-6}	20	90	37	
				3.3×10^{-5}	200	90	14	
				4×10^{-6}	110	90	29	
				3×10^{-6}	20	90	32	
				1.5×10^{-5}	30	90	19	
				3×10^{-6}	5	90	32	
				6×10^{-6}	30	100	26	
				1×10^{-6}	5	100	47	

8.	Japan	1961	7.0	5×10^{-7}	12	120	159	[25]
				5×10^{-7}	4	120	159	
9.	Japan	1961	7.0	2.5×10^{-6}	50	40	43	[25]
				5×10^{-6}	15	40	74	[25]
				1×10^{-6}	50	60	58	
				5×10^{-7}	15	60	34	
10.	Japan	1962	6.4	1×10^{-6}	20	35	70	[25]
				5×10^{-7}	7	35	88	
				1×10^{-6}	40	65	32	
				1×10^{-6}	3	65	70	
11.	Japan	1963	6.9	1.8×10^{-5}	180	90	44	[25]
				5×10^{-6}	60	90	67	
				3×10^{-6}	15	90	79	
				5×10^{-6}	180	80	67	
				7×10^{-6}	70	80	60	
				4×10^{-6}	15	80	72	
				2×10^{-6}	180	110	91	
				2×10^{-6}	60	110	91	
				1×10^{-6}	10	110	115	
12.	Japan	1969	6.5	5×10^{-7}	250	48	168	[25]
13.	Japan	1968	4.1	3×10^{-7}	0.42	10	16.5	[28]
14.	Japan	1968	5.3	4×10^{-7}	0.63	54	50	[28]
15.	U.S.S.R.	1957	4	5×10^{-7}	0.042	25	8	[25]
16.	U.S.S.R.	1958	4.7	3×10^{-7}	0.125	250	19	[25]
17.	Afghanistan	1959	5.5	3×10^{-6}	0.167	245	20	[25]
18.	U.S.S.R.	1956	6.0	9×10^{-8}	15	250	164	[25]
				5×10^{-8}	4	250	126	[25]
19.	U.S.S.R.	1967	5.5	3.5×10^{-6}	120	20	29	[26]
20.	U.S.S.R.	1965	6	2×10^{-7}	60	250	125	[27]
21.	U.S.S.R.	1967	5.8	1×10^{-7}	10	320	123	[27]
22.	U.S.S.R.	1965	7.5	5×10^{-7}	12	300	413	[29]
23.	U.S.S.R.	1964	4.5	7.5×10^{-8}	6	100	39	[29]
24.	U.S.S.R.	1963	6.3	5×10^{-8}	0.125	2800	269	[30]
				5×10^{-7}	0.125	600	124	[30]

that the presented estimates give the size not larger than that of the focal zone while the manifestation zone is often of greater dimensions (this is evident from the Table).

As already noted Fig. 5 also involves data on the phenomena that accompany the earthquake. Certainly, these phenomena cannot be considered precursors. However, their use in the plot is not meaningless. If we consider that the values of the changes in the deformation fields prior to and after the earthquake are quite close [37] then the comparison made is of interest.

As to the comparison of deformations accumulated in the preparation stage and those which appear during earthquakes we must mention the very interesting work of PRESS [38]. Using a dislocation model of the earthquake focal zone this author plotted the fields of theoretical deformations and tilts resulting from the earthquake. Comparison of our Figs. 2, 3 and 4 which show the deformation ϵ_{xx} with Fig. 5 from the work [38] reveals that according to their shape the field deformations are practically undistinguishable. As reported in [38] strains of 10^{-8} were distinctly recorded on Hawaii as a result of the Alaska earthquake of 27 March 1964. The earthquake magnitude was 8.6, the distance between the seismic station of Hawaii and the epicentre being as long as 4500 km. Our calculation for this magnitude and strain using equation (C) gives a distance of 4560 km. In other words we expect the pre- and co-seismic deformation fields to have very similar geometrical patterns and amplitudes. To our mind the problem discussed in this and preceding paragraphs is quite important and requires separate consideration.

4. Conclusion

The essence of the problem considered in this paper is to estimate the size of the effective precursor manifestation zone in general, i.e., the size independent of the physical nature of the precursor. Let us consider three theses:

(a) Because precursory phenomena appear not to be observed beyond the distance where $\epsilon = 10^{-8}$ (Fig. 5) we will consider the maximum radius the one for which $\epsilon = 10^{-8}$;

(b) Table 1 shows a satisfactory agreement between the theoretical results for deformations and tilts and the field observation data;

(c) When estimating the boundary of the precursor deformation zone we must probably bear in mind that it is difficult to separate the precursor deformations smaller than 10^{-8} against a background of tide deformation, especially for slow variations.

Hence we can draw the conclusion that a strain radius corresponding to a deformation of 10^{-8} may be regarded as a radius of the precursor manifestation zone.

Too big a radius increases the probability of erroneous prediction, especially for seismic active regions where a 'tight-packing' of the focal zones is observed.

Thus we propose to estimate the radius of the effective precursor manifestation zone by the formula

$$\rho = 10^{0.43M} \text{ km}$$

Appendix

Displacements of an elastic half-space with an inclusion

1. General formulae

An elastic half-space is exposed to the known system of mass forces and stresses at infinity. It is the initial state. When a weakened zone appears in the half-space then the new strains are established under the same boundary conditions. The difference between the new and initial strains represents the strains due to the inclusion appearance. They are detected by special devices on the half-space surface.

An approximate solution of the set problem by the perturbation method is given below.

Symbols

- x_i = Cartesian coordinates
- σ_{ij} = stress tensor
- f_i = mass forces
- u_i, v_i, w_i = displacements
- c_{ijkl} = elastic moduli tensor
- ε_{ij} = strain tensor
- n_i = guide cosines of the outer normal towards the surface
- δ = delta function
- δ_i^j = Kronecker's symbols
- ν = Poisson's ratio
- μ = shear modulus
- K = bulk modulus

Let us consider an inhomogeneous anisotropic elastic half-space $x_3 \geq 0$ (Fig. 1). The boundary $x_3 = 0$ is free of stresses. The values referring this state are designated by the upper index '0'. The displacements are described by a system of equations involving the equilibrium equations, the Hook's law and boundary conditions.

$$\begin{aligned} \sigma_{ij,j}^0 + f_i &= 0 & \sigma_{ij}^0 &= c_{ijkl}^0 u_{k,l}^0 \\ \sigma_{ij}^0 n_j &= c_{ijkl}^0 u_{ik,l}^0 n_j = 0 & \text{at } x_3 &= 0 \\ \sigma_{ij}^0(\infty) &= \sigma_{ij}^\infty. \end{aligned} \quad (1)$$

The solution of this problem is supposed to be known.

Here, and further, summing up is made according to the repeating indices. Comma in the index means the differentiation for instance

$$u_{k,i} = \partial u_k / \partial x_i.$$

Let us assume that the elastic moduli have undergone a change in a certain inner region V with the surface S . Then the new tensor of the elastic moduli can be presented as

$$c_{ijkl} = c_{ijkl}^0 + \alpha c'_{ijkl}. \quad (2)$$

We consider that

$$c'_{ijkl} \begin{cases} \equiv 0 & \text{at } x_i \notin V \\ \neq 0 & \text{at } x_i \in V \end{cases} \quad (3)$$

$$|c'_{ijkl}| \leq |c_{ijkl}^0|, \quad |\alpha| \leq 1.$$

The displacements of the half-space with an inclusion under unchanged boundary conditions are described by a system of equations

$$\begin{aligned} \sigma_{ij,j} + f_i &= 0 & \sigma_{ij} &= c_{ijkl} u_{k,l} \\ \sigma_{ij} n_j &= c_{ijkl} u_{k,l} n_j = 0 & \text{at } x_3 &= 0 \\ \sigma_{ij}(\infty) &= \sigma_{ij}^\infty \end{aligned} \quad (4)$$

It is assumed for simplicity that the mass forces remain unchanged.

As mentioned above the displacements w_i due to the inclusion appearance, i.e. the difference

$$w_i = u_i - u_i^0 \quad (5)$$

are of interest.

If we introduce the Hook's law in the equilibrium equations then the systems (1) and (4) can be formulated in terms of displacements.

The difference between these systems according to equations (2) and (5) gives a system for w_i

$$\begin{aligned} (c_{ijkl}^0 w_{k,l})_{,j} + \alpha (c'_{ijkl} u_{k,l}^0)_{,j} + \alpha (c'_{ijkl} w_{k,l})_{,j} &= 0 \\ c_{ijkl}^0 w_{k,l} n_j &= 0 \quad \text{at } x_3 = 0 \\ c_{ijkl}^0 w_{k,l} &\rightarrow 0 \quad \text{at infinity.} \end{aligned} \quad (6)$$

Let us seek for a solution to the problem (6) as power series

$$w_i = \sum_{m=0}^{\infty} \alpha^m w_i^{(m)}. \quad (7)$$

Substitution of (7) in (6) shows that $w_i^{(m)}$ can be determined from the following equations at zero boundary conditions

$$\begin{aligned} w_i^{(0)} &= 0 \\ (c_{ijkl}^0 w_{k,l}^{(1)})_{,j} + (c'_{ijkl} u_{k,l}^0)_{,j} &= 0 \\ (c_{ijkl}^0 w_{k,l}^{(m)})_{,j} + (c'_{ijkl} w_{k,l}^{(m-1)})_{,j} &= 0 \end{aligned} \quad (8)$$

$$(c_{ijkl}^0 w_{k,l}^{(m)})_{,j} + (c'_{ijkl} w_{k,l}^{(m-1)})_{,j} = 0 \quad (9)$$

$m = 2, 3, 4, \dots$

Let us introduce the Green's function v_i^r of the problem (1). v_i^r is a solution to the problem for a single force applied in the point x^0 in the direction of the axis x_r , i.e.

$$\begin{aligned} (c_{ijkl}^0 v_{k,l}^r)_{,j} + \delta_i^r \delta(x - x^0) &= 0 \\ c_{ijkl}^0 v_{k,i}^r n_j &= 0 \text{ at } x_3 = 0 \\ c_{ijkl}^0 v_{k,l}^r &\rightarrow 0 \text{ at infinity.} \end{aligned}$$

Then

$$w_r^{(1)} = - \iiint_V c_{ijkl}^0 u_{k,i}^0 v_{l,j}^r dV \tag{11}$$

$$\begin{aligned} w_r^{(m)} &= - \iiint_V c_{ijkl}^0 w_{k,i}^{(m-1)} v_{l,j}^r dV \\ &= \iiint_V (c_{ijkl}^0 v_{i,j}^r)_{,i} w_k^{(m-1)} dV - \iint_S c_{ijkl}^0 v_{i,j}^r n_l w_k^{(m-1)} dS \end{aligned} \tag{12}$$

at $m = 2, 3, 4$.

The solution to the problem is obtained with the equations (7), (11) and (12) at sufficiently low values of α .

The convergence region for series (7) depends upon the specific kind of the Green's function, region V and function c_{ijkl}^0 .

A simple but not strict evaluation of the series (7) convergence is possible. Let us assume that the elasticity moduli of the inclusion are similar to those of surrounding medium, i.e. $c_{ijkl}^0 = c_{ijkl}^*$. Then in (12) according to (10)

$$\begin{aligned} \iiint_V (c_{ijkl}^0 v_{i,j}^r)_{,i} w_k^{(m-1)} dV &= \iiint_V (c_{ijkl}^0 v_{i,j}^r)_{,i} w_k^{(m-1)} dV \\ &= - \iiint_V \delta_k^r \delta(x - x^0) w_k^{(m-1)} dV = -w_r^{(m-1)}. \end{aligned} \tag{13}$$

In equation (12) the underintegral expression of the integral on the surface represents a scalar product of the vectors $P_k^r = c_{ijkl}^0 v_{i,j}^r n_l$ and $w_k^{(m-1)}$. The vector P_k^r is the stress on the surface S . P_k^r is the surrounding medium response, distributed on S , to a single force δ_k^r acting in the volume V . Therefore

$$\iint_S P_k^r dS = \iint_S c_{ijkl}^0 v_{i,j}^r n_l dS = -\delta_k^r.$$

Let us assume that

$$\iint_S |P_k^r| dS \leq 2\delta_k^r.$$

This non-strict but rather intuitive assumption means the following. If a concentrated force is acting in direction x_r in volume V with surface S , then the sum of all moduli of the reactive forces projections applied to S from the surrounding medium does not exceed the double value of this concentrated force.

Now the surface integral in (12) permits us to evaluate

$$\begin{aligned} \iint_S c_{ijkl}^0 v_{i,j}^r n_l w_k^{(m-1)} dS &\leq \iint_S P_k^r w_k^{(m-1)} dS \leq |w_k^{(m-1)}| \iint_S |P_k^r| dS \\ &= 2|w^{(m-1)}| \delta_k^r = 2|w_r^{(m-1)}|. \end{aligned} \quad (15)$$

On the basis of (12) and according to (13) and (15) we obtain

$$|w_r^{(m)}| \leq 3|w_r^{(m-1)}|.$$

Hence series (7) converges at $\alpha < \frac{1}{3}$. At $\alpha \leq 0.1$ we can confine to the approximation assuming $w_r = w_r^{(1)}$.

Displacements of the homogeneous isotropic half-space surface

Thus we suggest that

$$w_r = -\alpha \iiint_V c_{ijkl}^0 v_{i,j}^r \mu_{k,l}^0 dV. \quad (16)$$

The main advantage of this formula is as follows: it describes the displacements for the inclusion of an arbitrary shape with arbitrary unhomogeneity and anisotropy when the Green's tensor for the initial medium is known. This tensor is known for instance for a homogeneous isotropic half-space. Let us remember that the displacement in equation (16) is calculated in the same direction and point where the single force of Green's tensor is applied. In particular, for estimation of the surface displacements it is necessary to know the solution for the force applied to the half-space boundary.

Let us consider a particular case. For a homogeneous inclusion and constant initial deformations

$$w_r = -\alpha c_{ijkl}^0 \mu_{k,l}^0 \iiint_V v_{i,j}^r dV.$$

For an isotropic medium

$$c_{ijkl}^0 \mu_{k,l}^0 = K' \varepsilon_{ij}^0 \delta_i^j + 2\mu' \left(\varepsilon_{ij}^0 - \frac{\delta_i^j}{3} \varepsilon_{nn}^0 \right) = \frac{K'}{K^0} \frac{\sigma_{ij}^0}{3} \delta_i^j + \frac{\mu'}{\mu^0} \left(\sigma_{ij}^0 - \frac{\sigma_{nn}^0}{3} \delta_i^j \right).$$

Therefore

$$w_r = -\alpha \left(\frac{K'}{K^0} \frac{\sigma_{ij}^0}{3} \delta_i^j + \frac{\mu'}{\mu^0} \left(\sigma_{ij}^0 - \frac{\sigma_{nn}^0}{3} \delta_i^j \right) \right) \iiint_V v_{i,j}^r dV. \quad (17)$$

Let \bar{v}_i be the tensor of displacements due to a single surface force. According [39]

$$\bar{v}_i = \frac{1}{4\pi\mu} \left(\frac{2(1+\nu)R + x_3}{R(R+x_3)} \delta_i^j + \frac{2R(\nu R + x_3) + x_3^2}{R^3(R+x_3)^2} (x_i - x_i^0)(x_j - x_j^0) \right),$$

$$\begin{aligned} \bar{v}_i^3 &= \bar{v}_3^i = \frac{1}{4\pi\mu} \left(\frac{x_3}{R^3} - \frac{1-2\nu}{R(R+x_3)} \right) (x_i - x^0), \\ \bar{v}_3^3 &= \frac{1}{4\pi\mu} \left(\frac{x_3^2}{R^3} + \frac{2(1+\nu)}{R} \right), \end{aligned}$$

where $i, r = 1, 2, R = \sqrt{(x_1 - x_1^0)^2 + (x_2 - x_2^0)^2 + x_3^2}$.

Let us assume that the half-space is subjected to constant shear stress, i.e. $\sigma_{12}^0 = \sigma_{21}^0 = \tau$; all the others $\sigma_{ij}^0 = 0$. If we consider that the cracks don't open in the weakened zone then $K' = 0$. This means the invariability of the bulk modulus. When $\mu' = \mu^0 = \mu$ we obtain from (17)

$$w_r(x^0) = -\alpha\tau \iiint_V (\bar{v}_{1,2}^3 + \bar{v}_{2,1}^3) dV. \tag{18}$$

Displacements w_r are calculated in elementary functions if V is a parallelepiped. For a region of a more complicated shape it is more convenient to calculate w_r approximately, replacing the underintegral function by its value in a certain inner volume point that in case of a symmetrical region coincides with the centre of the latter. Comparison with an exact value shows that the error in this approximate calculation is no more than several percents even for a zone close to the epicentre.

Let the inclusion centre be in the point $(0, 0, H)$. $x_1^0 = x, x_2^0 = y$ are the surface coordinates, $w_1 = u, w_2 = v, w_3 = w$ are the surface displacements, $r = \sqrt{x^2 + y^2 + H^2}$. By the approximate calculation of the integral (18) we obtain

$$\begin{aligned} u &= -\frac{\alpha V \tau y}{2\pi\mu r^2} \left(\frac{3x^2}{r^3} + \frac{1-2\nu}{(r+H)^2} \left(\frac{r^2-x^2}{r} - \frac{2x^2}{r+H} \right) \right), \\ v &= -\frac{\alpha V \tau x}{2\pi\mu r^2} \left(\frac{3y^2}{r^3} + \frac{1-2\nu}{(r+H)^2} \left(\frac{r^2-y^2}{r} - \frac{2y^2}{r+H} \right) \right), \\ w &= -\frac{\alpha V \tau xy}{2\pi\mu r^3} \left(\frac{3H}{r^2} - \frac{(1-2\nu)(2r+H)}{(r+H)^2} \right), \end{aligned} \tag{19}$$

where V is the inclusion volume.

Surface strains and tilts are

$$\begin{aligned} \epsilon_{xx} &= \frac{\partial u}{\partial x} = -\frac{\alpha V \tau 3xy}{2\pi\mu r^3} \left(\frac{2}{r^2} - \frac{5x^2}{r^4} + \frac{1-2\nu}{(r+H)^3} \left(\frac{2x^2}{r+H} - \frac{(y^2+H^2)(3r+H)}{r^2} \right) \right), \\ \epsilon_{yy} &= \frac{\partial v}{\partial y} = -\frac{\alpha V \tau 3xy}{2\pi\mu r^3} \left(\frac{2}{r^2} - \frac{5y^2}{r^4} + \frac{1-2\nu}{(r+H)^3} \left(\frac{2y^2}{r+H} - \frac{(x^2+H^2)(3r+H)}{r^2} \right) \right), \\ \epsilon_{xy} &= \frac{1}{2} \left(\frac{\partial u}{\partial y} + \frac{\partial v}{\partial x} \right) = -\frac{\alpha V \tau 1}{2\pi\mu r^3} \left(\frac{3(r^2-H^2)}{2r^2} - \frac{15x^2y^2}{r^4} + \frac{1-2\nu}{2(r+H)^2} \right) \\ &\quad \left(6r^2 - 4H^2 + \frac{4x^2y^2(5r+2H)}{r(r+H)^2} - \frac{(r^4+x^4+y^4-H^4)(5r+3H)}{r^2(r+H)} \right) \end{aligned} \tag{20}$$

$$\gamma_x = \frac{\partial w}{\partial x} = \frac{\alpha V_T}{2\pi\mu} \frac{y}{r^3} \left(\frac{3H}{r^2} - \frac{15x^2 H}{r^4} + \frac{1-2\nu}{(r+H)} \left(\frac{2x^2}{r+H} - \frac{(2r+H)(r^2-3x^2)}{r^2} \right) \right)$$

$$\gamma_y = \frac{\partial w}{\partial y} = \frac{\alpha V_T}{2\pi\mu} \frac{x}{r^3} \left(\frac{3H}{r^2} - \frac{15y^2 H}{r^4} + \frac{1-2\nu}{(r+H)^2} \left(\frac{2y^2}{r+H} - \frac{(2r+H)(r^2-3y^2)}{r^2} \right) \right).$$

Asymptotic expressions can be used at teleseismic distances and small depth ($H \ll r$). These expressions are obtained from (20) at $H = 0$. Let $\nu = 0.25$. Then

$$\begin{aligned} \varepsilon_{xx} &= -\frac{\alpha V_T}{2\pi\mu} \frac{3xy(y^2 - 4x^2)}{2r^7} \\ \varepsilon_{yy} &= -\frac{\alpha V_T}{2\pi\mu} \frac{3xy(x^2 - 4y^2)}{2r^7} \\ \varepsilon_{xy} &= -\frac{\alpha V_T}{2\pi\mu} \frac{r^4 - 15x^2 y^2}{2r^7} \\ \gamma_x &= -\frac{\alpha V_T}{2\pi\mu} \frac{y(4x^2 - r^2)}{r^6} \\ \gamma_y &= \frac{\alpha V_T}{2\pi\mu} \frac{x(4y^2 - r^2)}{r^6} \end{aligned} \quad (21)$$

The principal strains in polar coordinates ($x = r \cos \varphi$, $y = r \sin \varphi$) adopted from (21) are

$$\varepsilon_{1,2} = -\frac{\alpha V_T}{2\pi\mu} \frac{-9 \sin 2\varphi \pm \sqrt{675 \sin^4 2\varphi - 255 \sin^2 2\varphi + 64}}{8r^3} \quad (22)$$

and the maximum tilt γ is

$$\gamma = \sqrt{\left(\frac{\partial w}{\partial x}\right)^2 + \left(\frac{\partial w}{\partial y}\right)^2} = \frac{\alpha V_T}{2\pi\mu} \frac{1}{r^3}. \quad (23)$$

Equation (22) evidences that the values of the principal strains depend upon the direction. Extreme values are reached at $\varphi = \pm 45^\circ$. If $\varepsilon = \max(|\varepsilon_1|, |\varepsilon_2|)$ then from (22)

$$\varepsilon = \frac{31}{8} \frac{\alpha V_T}{2\pi\mu} \frac{1}{r^3} \quad (24)$$

Let ρ_ε be the maximum distance at which ε is observed. ρ_γ being the same distance for the tilts. For the teleseismic distance we obtain from (23) and (24)

$$\rho_\varepsilon = 0.853 \sqrt[3]{\frac{\alpha V_T}{\mu \varepsilon}}, \quad (25)$$

$$\rho_\gamma = 0.543 \sqrt[3]{\frac{\alpha V_T}{\mu \gamma}}. \quad (26)$$

REFERENCES

- [1] MIACHKIN, V. I., BRACE, W. F., SOBOLEV, G. A., and DIETERICH, J. H. (1975), *Two models for earthquake forerunners*, Pure appl. Geophys. 113 (1/2), 169-181.
- [2] BRADY, B. T., (1974), *Theory of earthquakes I. A scale independent theory of rock failure*, Pure appl. Geophys. 112 (47), 701-725.
- [3] BRADY, B. T. (1975), *Theory of earthquakes II. Inclusion theory of crustal earthquakes*, Pure appl. Geophys. 113 (1/2), 149-168.
- [4] HAYAKAWA, M. (1950), *The variations of the seismic wave velocity, geological survey of Japan report, special number, 7*.
- [5] NISHIMURA, E., KAMITSUKI, A. and KISHIMOTO, Y. (1960), *Some problems on Poisson's ratio*, in 'The Earth's Crust', Tellus, XII, 263.
- [6] SEMENOV, A. N. (1969), *The variation of the time ratio for transverse and longitudinal waves propagation prior to strong earthquakes*, Izv. USSR Acad. Sci., Physics of the Earth, No. 4.
- [7] NERSESOV, I. L. and KONDRATENKO, A. M. (1962), *Some results of studying compressional velocity variations and V_p/V_s in the focal zone*, Proceedings of the Institute of the Earth's Physics, USSR Acad. Sci. issue 25 (192) Moscow.
- [8] ESHELBY, I. D. (1957), *The determination of the elastic field of an ellipsoidal inclusion and related problems*, Proc. Roy. Soc. (London), Series A, 241, 376-396.
- [9] BEAUMONT, C. and BERGER J. (1947), *Earthquake prediction: modification of the Earth tide tilts and strains by dilatancy*, Geophys. J. Roy. astron. Soc. 39, no 1, 111-121.
- [10] BEAUMONT, C. and BERGER, D. (1974), *The Spectral tide analysis for earthquake prediction*, Proceeding of the symposium, Tashkent, 39-47.
- [11] DOBROVOLSKY, I. P. and MIACHKIN, V. I. (1976), 'The displacements of the surface of an elastic half-space with an inclusion,' in *Seismic Sounding of Focal Zones*, M., Nauka.
- [12] SHEBALIN, N. V. (1971), 'Comments on the prevailing periods, spectrum and focal zone of a strong earthquake,' in *Problems of Engineering Seismology*, vol. 14, Nauka, pp. 50-78.
- [13] DETT, J. S. (1973), *Earthquake lights: a review of observations and present theories*, Bull. Seismol. Soc. Amer. 63, no. 6.
- [14] CHALOV, P. I., TUZOVA, T. V. and ALECHINA, V. M. (1977), *Short variations in the radioisotopic parameters of fault waters and their correlation with the earthquake prediction*, Izv. USSR Acad. Sci., Physics of the Earth, No. 8.
- [15] CHI-YU, KING (1976), *Radon emanation on active faults*, Conference I. Abnormal animal behavior prior to earthquakes, Menlo Park, California, pp. 411-414.
- [16] IGUMNOV, I. V. (1977), All-Union symposium on the investigation of Gazli earthquakes. Izv. Arm. SSR Acad. Sci., vol. XXX, No. 1, 1977.
- [17] SULTAN-KHODJAEV, A. N., CHERNOV, I. G. and ZAKIROV, T. (1976), *Hydro-seismologic precursors of the Gazli earthquake*. DAN Uzb. SSR, No. 7.
- [18] American delegation, *Earthquake Research in China*, EOS, vol. 56, No. 11, 1975.
- [19] MIRZOEV, K. M., MELAMUD, A. S., et al. (1976), 'Search for spatial-time variations of the phenomena preceding the strong earthquakes,' in *Searches for Earthquake Precursors*, Tashkent, FAN.
- [20] OSIKA, D. A., MEGAEV, A. B., IVANOVSKAJA, T. S. and SAIDOV, O. A. (1977), *Hydrogeochemical anomalies preceding the tectonic earthquakes as consequence of focal zones formation processes*, DAN USSR, vol. 223, No. 1.
- [21] American delegation. Prediction of the Haicheng Earthquake. EOS, vol. 58, No. 5, 1977, pp. 236-272.
- [22] SOBOLEV, G. A. and MOROZOV, V. N. (1970), 'Local perturbations of the electric fields on Kamchatka and their correlations with the earthquake,' in *Physical Bases of Earthquake Prediction Methods*. Nauka, M., pp. 110-121.
- [23] ALTHAUSEN, A. M. (1975), 'Geo-electric effects of strong earthquakes,' in *Instrumental and Operational Developments in Geophysics*, Kiev, Naukova dumka.
- [24] YAMAZAKI, Y. (1975), *Precursory and coseismic resistivity changes*, Pure appl. Geophys. 113 (1/2), 219-227.

- [25] RIKITAKE, T. (1975), *Earthquake precursors*, Bull. Seismol. Soc. Amer. 65, No. 5, 1133–1162.
- [26] Latynina, L. A., KARMALEEVA, R. M. *et al.* (1974), 'Earth surface deformation before strong earthquake of the 3.10.1967,' in *Searches for Earthquake Precursors on Proving Grounds*. Nauka, M.
- [27] LATYNINA, L. A. and KARMALEEVA, R. M. (1970), *On certain anomalies in the variations of crustal strains before strong earthquakes*, Tectonophysics 9, No. 3–4, 239–247.
- [28] OZAWA, IRUO (1968), Observations of the Crustal strains of the time of earthquakes around Kyoto city, Special Contributions, Geophysical Institute, Kyoto University, No. 8, 91–108.
- [29] LATYNINA, L. A. and KARMALEEVA, R. I. (1970), 'Measurement of slow crustal movements as a method of predicting earthquakes,' in *Physical Basis of Earthquake Prediction*, M., Nauka, 52–50.
- [30] PANASENKO, G. D. (1964), *Observation of a tilt 'storm' as a precursor of a strong remote earthquake*, Izv. USSR Acad. Sci., Ser. Geophys., No. 10.
- [31] OSTROVSKY, A. E. (1970), 'Local changes in Earth tilts before strong near earthquakes,' in *Physical Basis of Earthquake Prediction*, M. Nauka.
- [32] RIKITAKE, T. (1968), *An approach to prediction of magnitude and occurrence time of earthquakes*, Tectonophysics 8, No. 2.
- [33] RIKITAKE, T. (1975), *Dilatancy model and empirical formulae for an earthquake area*, Pure appl. Geophys. 113, No. 1/2.
- [34] DAMBARA, T. (1966), *Vertical Movements of the earth's crust in relation to the Matsushiro earthquakes*, J. Geol. Soc. Jap. 12, No. 1.
- [35] YAMAUCHI, T. and YAMADA, M. (1975), *Detection of strain step associated with earthquake*, Zisin 28, No. 1.
- [36] ANDERSON, D. L. and WHITCOMB, J. H. (1975), *Time-dependent seismology*, J. Geoph. Res. 80, No. 11.
- [37] BENDEFY, L. (1966), *Elastic plastic and permanent deformations of the earth's crust in connection with earthquakes*, Suomalais tiedeakat Toimituks, ser. A 3, No. 90.
- [38] Press, F. (1965), *Displacements. Strains and Tilts at teleseismic distances*, Journal of Geophysical Research, 70, No. 10, 2395–2412.
- [39] LANDAU, L. D. and LIFSHITZ, E. M. (1965), *Theory of Elasticity*, Nauka, M.

(Received 15th August 1977)